The University of
Nottingham

UNITED KINGDOM · CHINA · MALAYSIA

Sanduleac, I. and Casian, A. (2015) Modeling of thermoelectric properties of n – type organic crystals of TTT(TCNQ)2: 3D physical model. Journal of Electronic Materials . ISSN 1543-186X

Access from the University of Nottingham repository:

http://eprints.nottingham.ac.uk/31269/1/Sanduleac_TTT%28TCNQ%292%2C%202015%2C%20accep.%20manuscr..pdf

Modeling of thermoelectric properties of n – type organic crystals of TTT(TCNQ)$_2$: 3D physical model.

Ionel Sanduleac and Anatolie Casian
Department of Computers, Informatics and Microelectronics,
Technical University of Moldova, Stefan cel Mare av. 168, Chisinau, Rep. of Moldova

Thermoelectric properties of quasi-one-dimensional TTT(TCNQ)$_2$ organic crystals are investigated in order to appreciate the prospect of using this compound as n – type thermoelectric material. A more complete three-dimensional (3D) physical model is elaborated. It takes into account two the most important interactions of conduction electrons with longitudinal acoustic phonons, the electrons' scattering on neighbor molecular chains, as well as the scattering by impurities and defects. The electrical conductivity, thermopower, the power factor, electronic thermal conductivity and the thermoelectric figure of merit in the direction along conductive molecular chains are calculated numerically for different degrees of crystal purity. It is shown that in stoichiometric compounds the thermoelectric figure of merit ZT remains small even after the increase of crystal perfection degree. The thermoelectric properties may be significantly enhanced by simultaneous increase of crystal perfection and of electron concentration. The latter can be achieved by additional doping with donors. For less pure crystals, the interaction with impurities predominates over the weak interchain interaction and the simpler one-dimensional (1D) physical model is applicable. When the impurity scattering is reduced, the interchain interaction begins to limit the carrier mobility and the application of the 3D physical model is required. The optimal parameters permitting to predict $ZT \sim 1$ are determined.

Key words: TTT(TCNQ)$_2$, electrical conductivity, Seebeck coefficient, power factor, thermal conductivity, thermoelectric figure of merit.

INTRODUCTION

Environmental problems facing humanity require a widespread implementation of renewable energy sources. Due to the abundance of low-level heat, thermoelectric devices are very promising to recover even a part of wasted energy. The search and investigations of high-efficient thermoelectric materials represent a priority purpose toward an eco-friendly technology for global and local power generation systems, cooling systems and for infrared sensors. In the last decade, thermoelectric properties of materials with complex crystalline structure, of low-dimensional systems, of superlattices with quantum dots and of nanostructured organic materials were successfully investigated in order to achieve high conversion efficiency.

In n – type clathrate crystal, thermoelectric figure of merit $ZT \sim 1 – 1.3$ was reported at $T = 800 – 1000$ K [1, 2]. In multiple-filled skutterudites, $ZT = 1.7$ at 850 K was realized [3]. High values of $ZT \sim 2.5$ were obtained also in low-dimensional systems, such as Bi$_2$Te$_3$/Sb$_2$Te$_3$ superlattices, and in superlattices with quantum dots PbTe/PbSe, with $ZT \sim 3$ at 600 K [4, 5]. New promising results were reported recently in Mg$_2$Sn$_{0.75}$Ge$_{0.25}$ compound – $ZT \sim 1.4$ at $T = 800$ K [6]. However, the wide scale implementation of thermoelectric devices based on inorganic materials requires very sophisticated production technology and expensive raw materials.

Recent investigations revealed that nanostructured organic materials might be very promising candidates as thermoelectric material. Their internal structure joins together the properties of low-dimensional systems and of complex compounds with much more diverse internal interactions. Moreover, thermoelectric properties are well-tunable by molecular chemistry methods. In DMSO – treated PEDOT: PSS, $ZT \sim 0.42$ was achieved by minimizing the total dopant volume [7]. High values of ZT were reported in mixed organic and inorganic compounds, such as hybrid material composed of nanoparticles of a polymer complex, carbon nanotubes and poly(vinyl chloride), $ZT \sim 0.3$ [8]. Important value, $ZT = 0.57$ at room temperature was measured in phenyl acetylene-capped silicon nano particles [9].

Earlier it was predicted theoretically [10] that in molecular structures consisting of nanowires of conducting polymers values of $ZT \sim 15$ may be achieved, and even $ZT \sim 20$ in charge transfer compounds [11], if the crystal purity is sufficiently high. In [12-14] the organic nanostructured crystals of tetrathiotetracene-iodide, TTT$_2$I$_3$, were proposed as prospect thermoelectric materials of p-type.

The aim of this paper is to propose and analyze the opportunity of organic crystal of TTT(TCNQ)$_2$ type as candidate for n – type thermoelectric material. A more complete three-dimensional (3D) physical model is elaborated, taking into account two the most important interactions of conduction electrons with longitudinal acoustic phonons, the electrons' scattering on neighbor

adjacent molecular chains, as well as the scattering by impurities and defects.

Electrical conductivity, thermopower, the power factor and the thermoelectric figure of merit in the direction of molecular conductive chains are modeled as function of Fermi energy in the frame of this physical model. The effect of electron scattering on adjacent molecular chains and the scattering on impurities are underlined. The criteria of applicability of the simpler one-dimensional (1D) physical model were established by analyzing crystals with different degree of purity. Further suggestions for increasing ZT are presented.

PHYSICAL MODEL OF THE CRYSTAL

Organic crystals of TTT(TCNQ)$_2$ have the aspect of dark-violet needles of length of 3 − 6 mm. The quasi one-dimensional internal structure consists of molecular chains arranged along one direction, further considered as x – axis of the Cartesian coordinate system. The lattice constants are c = 3.75 Å, b = 12.97 Å and a = 19.15 Å for x, y and z directions [15]. The overlap of HOMO (High Occupied Molecular Orbital) of nearest molecules along the TCNQ chain generates a narrow conduction band of width Δ = $4w_1$, where w_1 is the transfer energy of an electron from a given molecule to the nearest one in this direction. The parameter w_1 is not known for TTT(TCNQ)$_2$ crystals. The DFT calculations have given $\Delta \sim 0.7$ eV for TCNQ chains in TTT(TCNQ)$_2$ crystals, but this value was not applied in modeling of transport properties. A bandwidth Δ = 0.5 eV along the TCNQ chains was applied earlier for the modeling of electrical properties in a similar TTF-TCNQ organic crystal [16]. Therefore, we have taken the same value of 0.5 eV. A somewhat larger value of Δ would improve the thermoelectric properties. The overlap of π – orbitals of the nearest molecules in transversal to chain directions is insignificant, the transfer energies $w_2 = d_1 \cdot w_1$ and $w_3 = d_2 \cdot w_1$ are small and the transport mechanism is of hopping-type. The parameters $d_1 = d_2 = 0.015$ were estimated earlier for TTT$_2$I$_3$ crystals by comparing the experimental and numerical results of transversal electrical conductivity [17]. The internal structure of TTT(TCNQ)$_2$ crystals is similar to that of TTT$_2$I$_3$ and one can put $d_1 = 0.015$ and $d_2 = 0.01$ for y and z directions.

The energy of electrons is calculated in the approximations of tight-binding and nearest neighbors:

$$E(\boldsymbol{k}) = 2w_1[1-\cos(k_x c)] + 2w_2[1-\cos(k_y b)] + 2w_3[1-\cos(k_z a)], \quad (1)$$

here k_x, k_y, k_z are the projections of the quasi-wave vector $\boldsymbol{k}$ and the energy is measured from the bottom of the conduction band. The frequency of longitudinal acoustic phonons is:

$$\omega_{\boldsymbol{q}}^2 = \omega_1^2 \sin^2(q_x c/2) + \omega_2^2 \sin^2(q_y b/2) + \omega_3^2 \sin^2(q_z a/2), \quad (2)$$

where ω_1, ω_2 and ω_3 are limit frequencies and q_x, q_y, q_z are the projections of the quasi-wave vector $\boldsymbol{q}$. From the condition of quasi one-dimensionality it results that ω_2, ω_3 << ω_1. Only the longitudinal term in Eq.2 will be considered since the influence of the transversal terms on transport processes is very weak [18].

Two main electron-phonon interaction mechanisms are taken into account. The first mechanism is of the deformation potential type with coupling constants proportional to the derivatives of transfer energies with respect to the intermolecular distances, w_1', w_2', w_3'. The second mechanism is of polaron type. The lattice vibrations induce fluctuations of the polarization energy of molecules surrounding the conduction electron. The coupling constant is proportional to the mean polarizability of TCNQ molecules, α_0. To describe the ratio of amplitudes of the second mechanism to the first one, the parameters γ_1, γ_2 and γ_3 were introduced:

$$\gamma_1 = 2\alpha_0 e^2 /(w_1' c^5), \gamma_2 = 2\alpha_0 e^2 /(w_2' b^5),$$
$$\gamma_3 = 2\alpha_0 e^2 /(w_3' a^5). \quad (3)$$

The impurity and defect scattering processes are described by a dimensionless parameter D_0. It takes into account the point-like, electrically neutral and randomly distributed impurities (with concentration n_i) and thermally activated lattice defects (concentration n_d and activation energy E_0).

$$D_0 = (n_i I_i^2 V_{0i}^2 + n_d I_d^2 V_{0d}^2 e^{-2E_0/k_0 T}) M v_{s1}^2 / 4c^3 abw_1'^2 k_0 T . \quad (4)$$

Here I_i and I_d are the energy of interaction of the electron with an impurity and a defect within regions of volume V_{0i} and V_{0d}, respectively.

It is considered that a weak electric field and a weak temperature gradient are applied along conductive TCNQ chains. The kinetic equation is deduced using the two-particle temperature dependent retarded Green function. At room temperature the scattering of electrons on acoustic phonons can be considered as elastic. Furthermore, because of pronounced quasi-one-dimensionality of the crystal, w_2, w_3 << w_1, the transversal terms of Eq.1 in the law of energy conservation during the electron scattering were neglected too.

The expressions for electrical conductivity σ_{xx}, thermopower S_{xx}, power factor P_{xx}, electronic thermal conductivity κ_{xx}^e and thermoelectric figure of merit $(ZT)_{xx}$, have the form:

$$\sigma_{xx} = \sigma_0 R_0, \quad S_{xx} = (k_0 / e)(2w_1 / k_0 T)R_1 / R_0, \quad (5)$$
$$P_{xx} = \sigma_{xx} S_{xx}^2, \kappa_{xx}^e = 4w_1 (e^2 T)^{-1} \sigma_0 (R_2 - R_1^2 / R_0), \quad (6)$$
$$(ZT)_{xx} = 4w_1^2 \sigma_0 R_1^2 /(e^2 T R_0 (\kappa_{xx}^L + \kappa_{xx}^e)), \quad (7)$$

where k_0 is the Boltzmann constant, e – elementary charge, κ_{xx}^L - the lattice thermal conductivity. The coefficient σ_0 has the dimensionality of electrical conductivity:

$$\sigma_0 = (e^2 v_{s1}^2 M |w_1|^3 r) / 4\pi^3 \hbar abc(k_0 T)^2 w_1'^2, \quad (8)$$

here r = 2 is the number of molecular chains passing through the transversal section of the elementary cell, v_{s1} = $2.8 \cdot 10^3$ m/s is the sound velocity along the chains, M = $3.72 \cdot 10^5$ m_e (m_e is the electron rest mass) is the mass of TCNQ molecule, w_1' = 0.22 eVÅ^{-1}, κ_{xx}^L = 0.4 W/m·K. R_n are the dimensionless transport integrals:

$$R_n = abc \iiint d\boldsymbol{k} |\sin^3(k_x c)| \cdot [\varepsilon(\boldsymbol{k}) - \varepsilon_F]^n \cdot n_{\boldsymbol{k}} (1-n_{\boldsymbol{k}}) \cdot M_{\boldsymbol{k}}^{-1}$$

(9)

The expression under integral contains the dimensionless electron energy described in Eq. 1, $\varepsilon(\boldsymbol{k}) = E(\boldsymbol{k})/2w_1$ and the dimensionless Fermi energy $\varepsilon_F = E_F/2w_1$. Because of narrow conduction band, the integration is performed over entire Brillouin zone. n_k is the Fermi distribution function for electrons with energy $E(\boldsymbol{k})$ at room temperature. M_k describes the dimensionless mass operator of two-particle retarded Green function:

$$M_{\boldsymbol{k}} = [1 + \gamma_1 \cos(k_x c)]^2 + \{d_1^2[1 + 2\sin^2(k_y b) + 2\gamma_2 \cos(k_y b) + \gamma_2^2] + d_2^2[1 + 2\sin^2(k_z a) + 2\gamma_3 \cos(k_z a) + \gamma_3^2]\} / 8\sin^2(k_x c) + D_0.$$
(10)

Earlier, in the frame of the 1D model, only the first and the last terms in Eq. 10 were considered. For a narrow interval of energetic states near the resonant energy $\varepsilon_0 = (\gamma_1+1)/\gamma_1$ the electron-phonon interaction mechanisms partially compensate each other and M_k achieves a minimal value as function of k_x, leading to a pronounced maximum of the expression under integral in R_n, limited only by the scattering on impurities (D_0). Unlike the p-type crystals, now the maximum is placed in the upper half of the conduction band, $\varepsilon_0 > 1$. The model predicts high values for R_n, if the crystal purity is ultra-high. In the 3D model the weak interaction between adjacent molecular chains (second and third terms in Eq. 10) is also considered. Namely, this interaction begins to limit significantly the carrier mobility when the crystal purity is improved, leading to reasonable values for thermoelectric coefficients of ultra-pure crystals.

RESULTS AND DISCUSSIONS

The transport integrals (Eq. 9) can be calculated only numerically. The components of polarisability tensor of TCNQ molecule in vacuum are taken from DFT calculations [19], and the average value $\alpha_0 = 10$ Å^{-3} was estimated which leads to $\gamma_1 = 1.8$. Note that the results are not very sensitive to small variation of γ_1. The stoichiometric concentration of electrons in TTT(TCNQ)$_2$ crystals was estimated to $n = 1.1 \cdot 10^{21}$ cm^{-3} or $\varepsilon_F = 0.35$. The numerical calculations of thermoelectric coefficients (Eqs. 5 - 7) are performed for $D_0 = 0.1, 0.04, 0.02$ at room temperature.
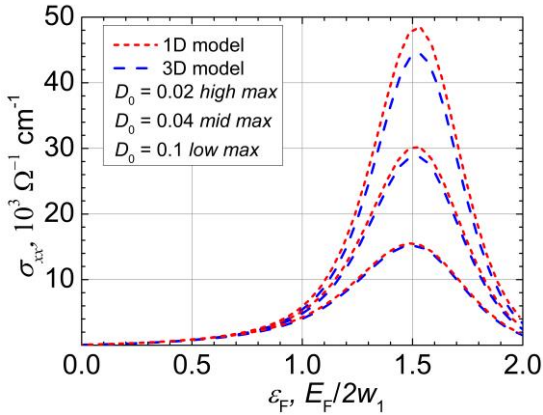

Fig.1. Electrical conductivity at 300 K as function of dimensionless Fermi energy.

The electrical conductivity as function of dimensionless Fermi energy is presented in Fig.1. The electrical conductivity of stoichiometric crystals ($n = 1.1 \cdot 10^{21}$ cm^{-3} or $\varepsilon_F = 0.35$) is low ($\sigma_{xx} \approx 0.46 \cdot 10^3$ Ω^{-1} cm^{-1}) and practically does not depend on the degree of crystal purity. However, it is observed that if the dimensionless Fermi energy is increased with respect to the stoichiometric value, the electrical conductivity grows significantly. From Fig.1. it is observed that σ_{xx} achieves $6.5 \cdot 10^3$ Ω^{-1} cm^{-1} for $D_0 = 0.02$, if the electron concentration is doubled ($n = 2.2 \cdot 10^{21}$ cm^{-3} or $\varepsilon_F = 1.05$). For purer crystals it is observed a small diminution of σ_{xx} in the 3D model as compared with the results of 1D model determined by the manifestation of the weak interchain interaction.

As it is seen from Fig.2, for stoichiometric crystals $S_{xx} \approx -120$ μV/K is expected. With the further increase of ε_F, or electron concentration, the absolute value of Seebeck coefficient firstly decreases, after that increases, achieves a maximum and decreases again up to zero. For $\varepsilon_F > 1.5$ the thermopower takes positive sign, meaning that the carriers become holes. When the concentration of electrons is increased by two times ($\varepsilon_F = 1.05$) with respect to the stoichiometric one, $S_{xx} = -105, -136, -160$ μV/K for $D_0 = 0.1, 0.04, 0.02$, very promising values.
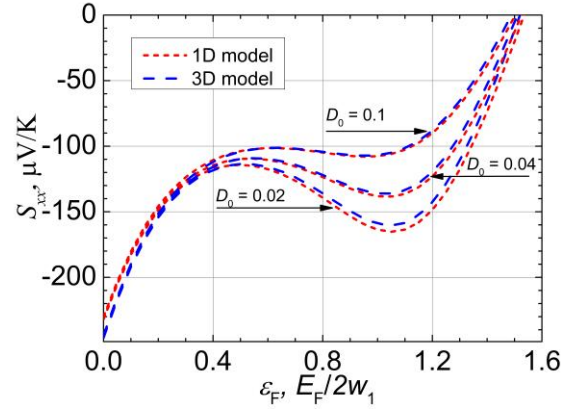

Fig.2. Thermopower at $T = 300$ K for different values of D_0.

The Seebeck coefficient of stoichiometric crystals is relatively high, but because of low electrical conductivity the power factor is very low, $P_{xx} \sim 6.5 \cdot 10^{-3}$ W/m·K^2 (Fig.3).
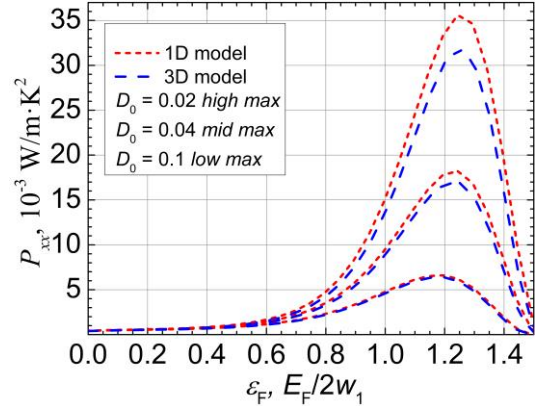

Fig.3. Power factor as function of dimensionless Fermi energy for different values of D_0.

The optimization of electron concentration (the increment of ε_F from 0.35 to 1.05) and further purification

procedure increases rapidly σ_{xx}, without diminishing S_{xx} too much. The power factor is growing significantly, up to $168 \cdot 10^{-3}$ W/m·K^2 (~ 4 times higher than in Bi$_2$Te$_3$). The deviations between the 3D and 1D models are more pronounced due to the cumulative contribution from the deviations of σ_{xx} and S_{xx}.

The electronic thermal conductivity κ_{xx}^{e} is shown in Fig.4. The interchain interaction is less manifested than in the case of electrical conductivity. The positions of maximums are little displaced toward lower values of ε_F with respect to the maximums of electrical conductivity (Fig.1). This phenomenon reveals the violation of the Wiedemann – Franz law.

The thermoelectric figure of merit ZT, achieves pronounced maximums for $\varepsilon_F \sim 1.1$ (Fig.5) and the largest contribution comes from the high values of the power factor, P_{xx}. In stoichiometric crystals $ZT = 0.02$ for $D_0 = 0.1$ and it remains small, even if the crystal purity is increased. This is explained by simultaneous increase of the electrical conductivity and of electronic thermal conductivity.
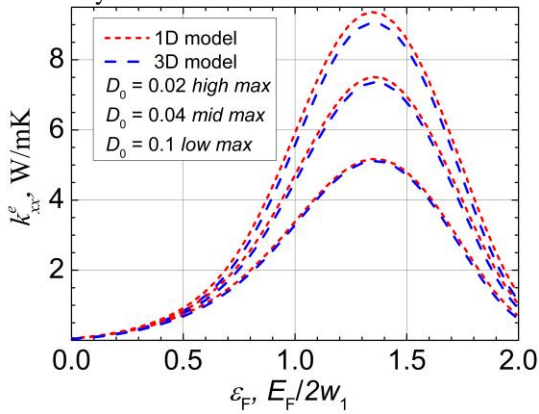

Fig.4. Electronic thermal conductivity κ_{xx}^{e}

as function of ε_F.

If the concentration of electrons is increased up to $2.2 \cdot 10^{21}$ cm^{-3}($\varepsilon_F = 1.05$), ZT grows rapidly, achieving values of 0.36, 0.57 and 0.75 for $D_0 = 0.1$, 0.04, 0.02, respectively.
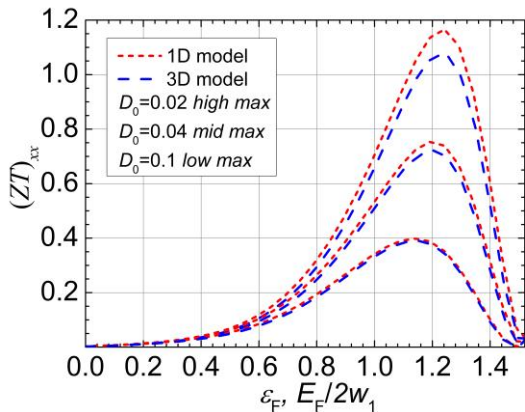

Fig.5. Thermoelectric figure of merit, ZT
as function of ε_F.

It is expected that $ZT \sim 1$ can be obtained in crystals with electrical conductivity $\sigma_{xx} \approx 12 \cdot 10^3$ Ω^{-1}cm^{-1}, thermal conductivity $\kappa_{xx}^{e} = 8.25$ W/m·K and thermopower $S_{xx} \approx -150$ µV/K.

If even an additional doping will somewhat increase the impurity scattering, values of $ZT \sim 0.8$ are predicted in considered crystals.

CONCLUSIONS

The modeling of thermoelectric properties in a rather realistic 3D physical model shows that organic crystal of TTT(TCNQ)$_2$ may be good candidate for n – type thermoelectric material, if the optimization of internal parameters is performed. Values of $ZT \sim 1$ are expected for crystals with electrical conductivity $\sigma_{xx} \approx 12 \cdot 10^3$ Ω^{-1} cm^{-1}, thermal conductivity $\kappa_{xx} = 8.25$ W/m·K and thermopower $S_{xx} \approx -150$ µV/K. The optimization procedure consists in an additional doping with donors and further purification of the crystal, in order to achieve the needed electrical conductivity. The influence of weak interaction between the adjacent molecular chains is analyzed by comparing deviations between the results of 1D and 3D physical models. It was observed that for not very pure crystals with $\sigma_{xx} < 22 \cdot 10^3$ Ω^{-1}cm^{-1} the simplest 1D model is applicable. For purer crystals the 3D model should be used.

REFERENCES

1. T. Takabatake, S. Koichiro, T. Nakayama, Rev. Mod. Phys. **86**, 669 (2014).
2. M. Rowe, L. Zhou, D. Banerjee, J. Electron Mater. **44**, 425 (2015).
3. S. Xun, J. Yang, J. Salvador, J. Am. Chem. Soc. **133**, 7837 (2011).
4. R. Venkatasubramanian, E. Siivola, T. Colpitts, B. O'Quinn, Nature **413**, 597 (2001).
5. T. C. Harman, P. J. Taylor, M. P. Walsh, B. E. LaForge, Science **297**, 2229 (2002).
6. L. Weishu, H.S. Kim, S. Chen, Q. Jie, Proc. Natl. Acad. Sci. U.S.A. **112**, 3269 (2015).
7. G. Kim, L. Shao, K. Zhang, K. P. Pipe, Nat. Mater. **12**, 719 (2013).
8. N. Toshima, K. Oshima, H. Anno, Adv. Mater. **27**, 2246 (2015).
9. S. P. Ashby, J. García-Cañadas, G. Min & Y. Chao, J. Electron Mater. **42**, 1495 (2013).
10. Y. Wang, J. Zhou, and R. Yang., J. Phys. Chem. C **115**, 24418 (2011).
11. A. Casian, in: Thermoelectric Handbook, Macro to Nano, Ed. by D. M. Rowe, CRC Press, 2006, Chap.36.
12. A. Casian, I. Sanduleac, J. Electron Mater. **43**, 3740 (2014).
13. I. I. Sanduleac, A. I. Casian, J. Pflaum, JNO. **9**, 247-252 (2014), open access.
14. A. Casian, J. Pflaum, I. Sanduleac, JTE. (2015), in press.

4

15. L. Buravov, O. Eremenko, R. Lyubovskii, & E. Yagubskii, J. Exp. Theor. Phys. Lett. **20**, 208 (1974).
16. 1. E. Conwell, Phys. Rev. B **22**, 1761 (1980).
17. I. Sanduleac, JTE **4**, 50 (2014).
18. I. Sanduleac, Moldavian Journal of the Physical Sciences, in press. (2015).
19. L. Cano-Cortes, A. Dolfen, J. Merino, Eur. J. Phys. B **56**, 173 (2007).